Turmeric Phyto-nanoparticle: enhanced cellular bioavailability and anti-inflammatory effect in human monocyte / macrophage model

Author list:

Bienvenue C. Habiyambere[1,4], Anirban Ghosh[2], Kenneth D'Souza[3,4], Victoria Northrup[1,4], Minji Kim[1,4], Victoria L. Nelson[1,4], Kyle R.D. Wells[1,4], Tori Nelson[1,4], Keith R. Brunt[1,4]

[1] Department of Pharmacology, Dalhousie Medicine New Brunswick, New Brunswick, Canada

[2] Pividl Bioscience Inc, New Brunswick, Canada

[3] New Brunswick Heart Center, New Brunswick, Canada

[4] IMPART investigator team Canada (https://impart.team/)

Correspondence: Keith R. Brunt (keith.brunt@dal.ca) or Anirban Ghosh (anirban@pividl.com)

Abstract: The poor bioavailability of curcuminoids remains a major challenge due to their hydrophobic nature, which is currently being addressed through advancements in nano- and micro-emulsion technologies. Curcuminoids and other water-insoluble phyto-polyphenols offer significant health benefits as anti-inflammatory, antioxidant, anticancer, radioprotective, and neuroprotective agents. Conventional emulsion-based delivery systems; such as liposomes, micelles, or solid lipid particles; rely on various emulsifying surfactants and/or excipients, some of which may pose health risks. In this study, a novel class of all-natural, additive-free, oil-free, and emulsion-free turmeric phyto-nanoparticles (TPNPs, developed directly from turmeric rhizomes) were evaluated in human monocyte/macrophage cell-line model to assess cellular bioavailability kinetics and anti-inflammatory activity. TPNPs are enriched with curcuminoids (24.85% by mass), form a homogeneous particle population, exhibit higher antioxidant capacity, and demonstrate significantly improved cellular uptake in both monocytes and macrophages compared to standard purified curcuminoids, which

also formed nanoparticles in cell culture media. The pharmacodynamic anti-inflammatory effect of TPNPs was evidenced by increased expression of the cytoprotective enzyme heme oxygenase-1 (HMOX1), and a more effective reduction in lipopolysaccharide (LPS)-induced tumor necrosis factor-α (TNF-α) secretion than that achieved by standard purified curcuminoids. TPNPs may thus serve as a safe and effective curcuminoid nanocarrier.

Keywords: Curcumin, Curcuminoids, turmeric Phyto-nanoparticle (TPNPs), monocyte, macrophages, THP-1.

1. Introduction:

In pharmacokinetics, bioavailability refers to the fraction of an administered dose of active pharmaceutical ingredients (APIs) that enters the systemic circulation, as well as the rate at which this occurs. The kinetics of absorption, metabolism, and elimination are key factors that influence effective bioavailability and the maintenance of steady-state plasma concentrations. Preclinical studies frequently utilize *in vitro* models that assess cellular bioavailability and relevant signaling pathways to predict and validate the therapeutic efficacy of APIs.

Curcuminoids, a group of bioactive polyphenols derived from turmeric (*Curcuma longa* rhizomes), have garnered significant attention owing to their demonstrated therapeutic benefits in both disease prevention and treatment [1]. Nevertheless, their clinical utility is challenged by suboptimal pharmacokinetic properties, including low aqueous solubility, poor absorption, and rapid metabolic turnover. Curcuminoids are known for their potent anti-

inflammatory and antioxidant actions, rendering them promising agents for the management of chronic inflammatory diseases, cardiovascular conditions, and cancer [2]. While inflammation is a fundamental immune defense against injury and infection, persistent low-grade inflammation contributes to tissue damage and underpins many chronic disease states [3]. Environmental toxins, unhealthy lifestyles, psychosocial stress, and obesity are key drivers of such chronic inflammation. For instance, free radicals (FRs), highly reactive molecular species produced under physiological and pathological conditions, can cause significant cellular injury. When produced in excess and not neutralized by intrinsic antioxidant mechanisms, FRs can impair membranes, proteins, and DNA, initiate mutations, and drive apoptotic pathways. Curcuminoids exhibit cytoprotective effects via multiple molecular mechanisms: (i) scavenging of FRs [4]; (ii) induction of endogenous antioxidant enzymes and pathways, such as Heme Oxygenase-1 (HMOX1) [5]; and (iii) suppression of inflammatory cytokines, including TNF-α [6]. Numerous peer-reviewed studies have highlighted the beneficial role of curcuminoids in contexts such as inflammation, metabolic dysfunction, tissue repair, liver and cardiac toxicity, inflammatory bowel conditions, drug resistance, and immune modulation [7, 8]. Additionally, curcuminoids have been linked to beneficial modulation of the gut microbiota and enhancement of gastrointestinal barrier function [9 ,10]. Consequently, improving the pharmacokinetics of curcuminoids through novel delivery methods is critical to unlocking their full therapeutic potential across diverse chronic and inflammatory conditions. Ongoing research continues to elucidate their diverse molecular mechanisms of action, reinforcing their value in modulating inflammatory, oxidative, and immune pathways. Curcuminoids inhibit the production of pro-inflammatory mediators such as IL-1β, IL-6, and TNF-α, and reduce the expression of adhesion molecules and inflammation-associated enzymes. Furthermore, they

downregulate NF-κB signaling, a central mediator of inflammation and tumorigenesis [11]. Curcuminoids also influence cell-cycle regulators, inhibit epithelial-mesenchymal transition relevant to metastasis [12], and activate autophagy [13], a critical pathway for cellular maintenance and turnover. They exert effects on Toll-like receptors (TLRs), restore gut microbiota balance, and improve intestinal integrity, offering benefits in immune and inflammatory disorders [14, 15]. In neurodegenerative contexts, curcuminoids have been found to provide neuroprotection [16], partly through inhibiting protein misfolding, regulating chaperones like heat shock proteins, and promoting autophagic flux.

Human Heme Oxygenase-1 (HMOX1) is a crucial enzyme in the cellular stress response and plays a central role in immunological and inflammatory homeostasis, particularly in macrophages. It mediates the transition between pro-inflammatory M1 and anti-inflammatory M2 macrophage phenotypes. HMOX1 catalyzes the degradation of heme into biliverdin, carbon monoxide, and free iron—all of which possess cytoprotective and anti-inflammatory properties in various cell types, including monocytes/macrophages. Biliverdin is subsequently converted into bilirubin, a potent antioxidant capable of mitigating oxidative stress by neutralizing reactive oxygen species (ROS). By promoting M2 polarization, HMOX1 contributes to inflammation resolution and tissue repair [17]. Its expression is associated with improved cardiovascular profiles and reduced atherosclerotic risk. Tumor necrosis factor-alpha (TNF-α) is a pleiotropic cytokine and key orchestrator of inflammatory responses, produced primarily by cells of the monocytic lineage such as macrophages, Langerhans cells, Kupffer cells, and microglia, in addition to other immune cells like neutrophils and T cells [18]. Elevated TNF-α levels are implicated in diseases such as rheumatoid arthritis, inflammatory bowel disease, psoriatic arthritis, and psoriasis, where it contributes to tissue pathology and

chronic inflammation. TNF-α also disrupts endothelial cell function, contributing to vascular pathologies. Curcuminoids have been shown to induce HMOX1 expression [19, 20], reduce TNF-α–driven inflammatory signaling in endothelial cells [21], and support anti-inflammatory M2 macrophage polarization [22], collectively contributing to immunomodulation and inflammation control. These findings support the potential of curcuminoids in naturally regulating TNF-α levels and highlight the therapeutic relevance of targeting HMOX1 and TNF-α in inflammation and oxidative stress-driven conditions.

Despite the broad therapeutic potential of curcuminoids, their clinical advancement has been hindered by challenges in bioavailability, primarily due to poor solubility and rapid hepatic metabolism. A wide array of curcuminoid encapsulation / formulation platforms—such as liposomes, micelles, and lipid-based nanoparticles—have been developed to enhance bioavailability, stability, and biocompatibility [23 , 24]. Over recent decades, an increasing number of human clinical trials have examined multiple orally delivered curcuminoid formulations for disease treatment, with promising results across a range of conditions [25, 26, 27,28]. Approximately half of these trials focus on diseases involving chronic inflammation, including metabolic and musculoskeletal disorders, and have generally reported favorable therapeutic outcomes.

However, current nano- and microencapsulation systems rely on specialized emulsifiers and surfactants, many of which are associated with toxicity risks. Surfactants are amphiphilic molecules comprising hydrophobic tails and hydrophilic heads, and are categorized into non-ionic, anionic, cationic, or amphoteric types. The majority are synthetic or chemically modified substances. Increasing evidence links dietary emulsifiers and surfactants—used as stabilizers

or delivery agents—to adverse health and environmental effects, particularly in the context of prolonged, low-dose exposure. Notably, such agents have been shown to alter gut microbiota composition [29, 30], contribute to metabolic disorders such as cardiovascular disease, hypertension, and type 2 diabetes [31,32, 33], and impair gut epithelial integrity [34, 35], all mechanisms associated with TNF-α dysregulation. Chronic use may also entail substantial long-term health burdens [36]. Animal studies further suggest that certain emulsifiers can alter gene expression in brain cells, influencing stress response and blood pressure regulation [37, 38]. Non-ionic surfactants like Polysorbates (Tweens), among the most widely used, have been reported to cause cytotoxic and genotoxic effects *in vitro* [39, 40, 41, 42]. Cationic surfactants—such as cetyltrimethylammonium bromide, dimethyl-dioctadecylammonium bromide, and cetylpyridinium chloride—are essential in nucleic acid delivery systems but are also associated with significant cytotoxic potential [43, 44, 45]. Polyethylene glycol (PEG), another commonly used polymer surfactant, is broadly approved for use in food, cosmetics, and pharmaceuticals due to its biocompatibility and favorable pharmacokinetic properties [46]. Nonetheless, frequent exposure to PEG-containing products has been shown to elicit anti-PEG antibody responses in the general population [47], raising concerns about immunogenicity due to cumulative exposure through food, drugs, and vaccines.

In this study, we evaluate the bioavailability and anti-inflammatory potential of a novel, all-natural Turmeric Phyto-Nanoparticle (TPNP) formulation that is free from emulsifiers, surfactants, and carrier oils. Importantly, the entire composition of TPNP is derived from the whole turmeric rhizome, ensuring a bio-native micelle matrix devoid of synthetic additives or delivery agents.

2. Materials and method:

2.1 THP-1 cell culture: THP-1 human monocytes were expanded from frozen stocks originally purchasedfrom the American Type Tissue Culture Collection (ATCC) using plating media containing Roswell Park Memorial Institute-1640 (RPMI-1640; ThermoFisher Scientific CAT#A1049101) supplemented with 10% FBS (ThermoFisher Scientific CAT#12483020). Cells were maintained at 37oC and the media was replaced every 3-4 days. THP-1 proliferative monocytes remain as suspension of cells which were differentiated into adherent macrophages by diluting 10nM PMA (VWR, CAT#10187-494) directly in RPMI1640-10% FBS media. After treatment with PMA, media was replenished with PMA-free RPMI-1640-10% FBS media and incubated for 24hrs for differentiation. Treatments were then applied to monocytes and differentiated macrophage cell cultures in RPMI-1640 with 0.5% FBS.

2.2 Turmeric phyto-nanoparticle and control standard curcuminoids spontaneous aggregating particles: Turmeric phyto-nanoparticles (TPNP) were manufactured and supplied by Pividl Bioscience Inc. (Canada) as sterile aqueous suspension in 0.1x PBS (pH7.4) with 15% ethanol. TPNP are manufactured as bio-native micelle-type structures enriched with curcuminoids directly from turmeric rhizomes. The knowhow of TPNP manufacturing remains with the supplier. The standard curcumin used was purchased from Sigma [curcumin (C1386) powder].

Curcuminoids Standard Spontaneous Aggregating Particle (CSAP) formation in cell treatment media: the cell culture media used for treatment was RPMI-1640 supplemented with 0.5%

FBS. The latter media was spin-filtered (300 kDa filters) to remove particles like extracellular vesicles and protein aggregates present in FBS. Sigma curcumin powder was dissolved in 95% ethanol to make a stock solution (1.5 mM), which was used to further to prepare 50 µM curcuminoids equivalent CSAP in 300 kDa-filtered RPMI-1640 (0.5% FBS) media following incubation at 37 °C for 30 min with intermittent mixing and CSAP colloidal formation was observed. Similarly, CSAP formation in aqueous media of RPMI-1640 and 0.1x PBS, with or without 0.5% FBS were evaluated.

2.3 Nanoparticle characterization: Nanoparticle properties were determined using dynamic light scattering (DLS) and Tunable Resistive Pulse Sensing (TRPS) using Zetasizer Nano ZSP (Malvern) and qNano Gold (Izon) instruments respectively. TPNP were diluted 10 times or 15 times (in 0.1x PBS) and 10,000 times (in deionized water) for DLS and TRPS respectively to measure hydrodynamic diameter, count per ml and zeta potential.

2.4 Total curcuminoid quantitation using fluorescent spectroscopy and HPLC:

For fluorescent spectroscopy Synergy H4 Hybrid Reader (Biotek) was used. standard curcumin (Sigma) powder was measured and dissolved in 80% ethanol to make two stocks of 1.5 mM curcuminoids equivalent and serially diluted to 1000 nM,100 nM, 10 nM, and 1 nM in 80% ethanol to produce a standard curve with excitation at 420 nm and emission capture at 570 nm. TPNP samples were 3125-times diluted in 80% ethanol for the above quantitation. The fluorescent spectroscopy method was further validated with HPLC. To quantitate if three curcuminoids present in standard curcumin (Sigma) powder and TPNP formulation using HPLC, a ternary isocratic chromatographic method, coupled with optical diode array detection monitoring compound-specific wavelengths was used. In brief, stock solutions of the three individual curcuminoid standards (Curcumin, Desmethoxycurcumin and

Bisdemethoxycurcumin) at 1000 µg/mL were prepared in acetone, followed by diluted to 100 µg/mL (100 ppm) in acetonitrile and used to perform HPLC method optimization and to acquire optical diode array detector (DAD) spectra for the individual compounds. Further validation was performed by mixing three individual curcuminoids standards at 100 µg/mL and used for daily instrument calibration. The three reference standards obtained for this work had a purity equal to or greater than 98%. The chromatographic separation of the three curcuminoids was optimized using an isocratic method, which proved to be the most reliable. A final ternary isocratic method consisting of 30% acetonitrile, 25% methanol and 45% water, supplemented with 0.1% phosphoric acid was employed to separate the three curcuminoids sufficiently and to minimize secondary interaction of the curcuminoids with the nanocarrier. DAD setting was scanning range 210-800 nm, with 1 nm increments, data acquisition was done with Masslynx 4.2 with TargetLynx.

2.5 Transmission electron microscopy (TEM): TPNP was directly deposited as 5 or 10 µl onto 200 mesh formvar/carbon grids and allowed to incubate at room temperature for 10 minutes before removing the excess liquid by wicking with filter paper. The grid was then sequentially washed twice for two minutes by floating sample-side down on two separate 100 µl of ddH2O (0.22 µm filtered) droplets on parafilm. Contrast staining was done by floating sample-side down on 1% uranyl acetate (Fisher Scientific Company) droplet for 1 minute. Grids were imaged with a STEM3+ detector on a Scios 2 DualBeam (Thermo Scientific) at 80,000 x magnification and 30 kV accelerating voltage. Preparation, imaging, and processing were conducted at the Microscopy and Microanalysis facility at the University of New Brunswick, Fredericton campus (Biology Department).

2.6 Antioxidant capacity: The total antioxidant capacity was determined according to the recommended procedures of the manufacturer of the Ferric Reduction Antioxidant Potential (FRAP) assay kit (ThermoFisher, Cat # EIAFECL2). In brief, Ferrous chloride [10mM] was diluted in 1X acetate buffer to prepare Fe2+ standards of 0, 31.25, 62.5, 125, 250, 500 and 1000 (µM) by serial dilution. All samples were diluted in 1X assay buffer. An ascorbic acid positive control was diluted to 250 µM as assay control to find if the chemistry worked. Fresh stock of 62.5 µM of each of Curcumin (Sigma), N-Acetyl-L-Cysteine (NAC, Amresco Cat#0108-25G) and gallic acid (GA) were made in 1X assay buffer as references. A fresh Fe2+ standard curve was prepared for each assay. The absorbance was read at 560nm using a Synergy H4 Hybrid Reader (Biotek).

2.7 Immunoblotting and Confocal microscopy: The immunoblotting method were followed from our previous publication [48] following treatments as indicated in the result sections. Confocal microscopy was also followed from previous publication [49] with minor modifications. In brief, THP-1 cells were seeded at a density of $1x10^5$cells/well on sterilized coverslips placed in 6-well plates and differentiated to macrophages. Hoechest 33258 (ThermoFisher, Cat#62249) was used at a 0.5µL:10 000µL dilution to stain nucleus for 1 minute and finally mounted / sealed on a microscope slide using PermaFluor mounting media (ThermoFisher, Cat#TA030FM).

2.8 Flow cytometry: THP-1 cells were treated as indicated in the result sections followed by fixing in 2% formalin in FACS buffer (0.1% BSA in 1x PBS) and subsequently washed twice with 1X PBS. Cells were then gated and stored (75,000 cells) using the GalliosTM 10-color Flow Cytometer (Beckman Coulter) and curcuminoid fluorescence was assessed in the FL2+ channel.

2.9 Cell viability assay: Cell viability assay was performed as per supplier recommendation of PrestoBlueTM Cell Viability Reagent (Invitrogen). Spectral fluorescence was measured using a Synergy H4 Hybrid Reader (Biotek) with excitation and emission wavelengths of 560 and 590 nm respectively.

2.10 ELISA: For TNF-α measurement in the cell culture media ELISA MAX^{TM} Standard-set kit (BioLegend) was used according to the manufacturer's protocol and absorbances were read using a Synergy H4 Hybrid Reader (Biotek).

3. Results

3.1. Turmeric Phyto-Nanoparticle (TPNP) characterization:

Each batch of TPNP was stored at 4°C to 8°C for three months and batch-to-batch hydrodynamic diameter (nm) and Polydispersity index (PDI) were verified after 10X dilutions in 0.1xPBS (Table 1) using dynamic light scattering (DLS). The above TPNPs were also dried using vacuum assisted freeze-drying (-40°C) with sucrose (10% w/v, as cryo-drying excipient) to a powder form (Figure 1A) and immediately sealed in multiple air tight containers, stored at room temperature in dark and dry environment. For rehydration, 0.1g of the dried TPNPs was dissolved in 1 mL of distilled water followed by a further 10X dilution in water (Figure 1B, Table 1). The freeze-dried powders were found to increase their size after rehydration but still maintained excellent homogeneity (Table-1) for up to 2 years. To visualize TPNPs morphology, Transmission Electron Microscopy (TEM) was performed (Figure-1C) and these phyto-nanoparticles were found to be spherically shaped. The average hydrodynamic diameter distribution of the TPNP shown in Figure-1D was measured using DLS after 10X dilution in 0.1xPBS and

a single peak (177 ± 0.964 nm) was observed, demonstrating particle size homogeneity (PDI= 0.111). The uniformity of particle population was also shown by correlation coefficient curve (Figure- 1D insert).

Formulation type	Time	Average hydrodynamic size (d.nm)	PDI
Hydrated TPNP	Batch #1	173 ± 0.762	0.131
	Batch #2	177 ± 0.964	0.111
Freeze-Dried TPNP (Batch #1)	6 months	214 ± 2.86	0.055
	9 months	235 ± 1.76	0.128
	24 months	223 ± 3.76	0.254

Table-1

Table-1: Hydrodynamic diameter (nm) and polydispersity index (PDI) of TPNP using dynamic light scattering measurements for different batches of liquid samples and rehydrated freeze-dried samples at different time points

TPNPs was also analysed using Tunable Resistive Pulse Sensing (TRPS) based particle analysis. Figure-1E shows TRPS of TPNPs diluted 10,000X in deionized water and found to contain about 9.58 x 10^{10} particles / mL counts with mean particle diameter 176 ± 67.9 nm whereas mode particle diameter was 132 nm.

Both DLS and TRPS were also used to measure the surface charge (mV) or Zeta potential of those particles. In DLS, TPNP showed a net surface charge (zeta potential) of -0.189 mV in an ionic environment 0.1xPBS (15X dilution in 0.1xPBS) (Figure-1F).

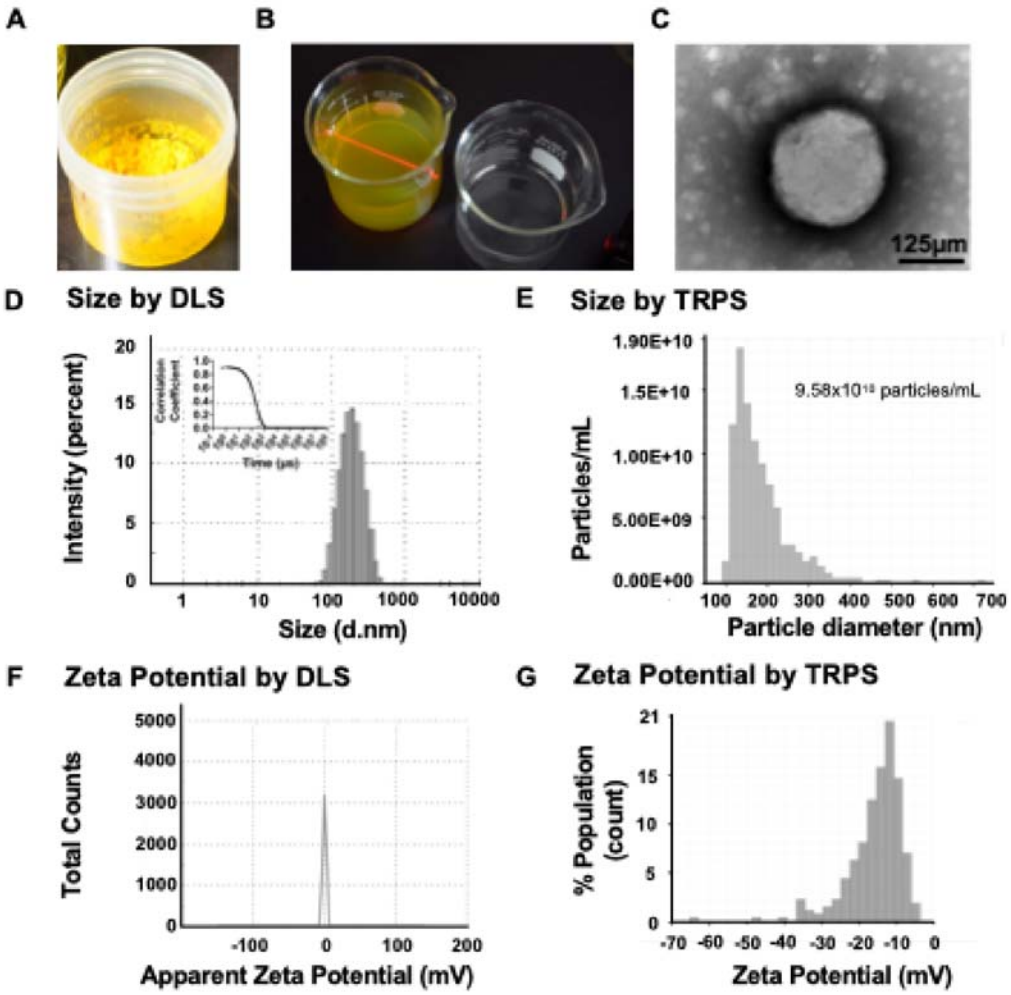

Figure-1

Fig-1: (A) Freeze dried TPNP stored at room temperature, (B) Rehydration of Freeze dried TPNP in water (right beaker: water, left beaker: rehydrated TPNP, red leaser source bottom right red-dot), (C) A representative image of TPNP using Transmission Electron Microscopy, (D) Particle size distribution of TPNP using Dynamic Light Scattering (DLS) where insert represent its monodisperse correlation coefficient curve, a measure of decaying exponential function, (E) Particle size distribution of TPNP using

Tunable Resistive Pulse Sensing (TRPS), (F) Zeta potential of TPNP using DLS, (G) Zeta potential of TPNP using TRPS.

Diluted TPNPs (10,000X dilution in deionized water) was used to measure zeta potential using TRPS producing a mean value of -15.0 mV and mode -11.7 mV, respectively (Figure-1G). The discrepancies of zeta potential value of DLS data in comparison to TRPS data may be due to the presence of sufficient buffering salt from 0.1x PBS (pH7.4) used as diluent in DLS which may neutralize charges, whereas 10,000X dilution in deionized water did not have sufficient buffering salt.

3.2 Curcuminoids Standard Spontaneous Aggregating Particle (CSAP) formation in cell treatment media:

Curcuminoids are poorly water soluble and form unstable colloidal particles or aggregates in aqueous media like PBS and RPMI-1640 cell growth media [50]. Thus, we tested whether curcumin used here as pharmacological reference standard could produce particles by spontaneous aggregation in cell treatment media as described in the method section. Hydrodynamic diameter of the CSAP formed in the cell treatment media (RPMI-1640 + 0.5% FBS) exhibited an average size of 122.1 ± 0.6 nm and PDI of 0.259 in DLS measurements (Figure S1A). To find if the same stock of Sigma curcumin when added to different aqueous media produce same or different sized spontaneous aggregations, the following conditions were verified using DLS and observed that: (i) in RPMI-1640 without any FBS, average diameter was 940.4 ± 98.52 nm and PDI=0.214 (Figure S1B), (ii) in 0.1x PBS with 0.5% FBS, average diameter was 120.2 ± 1.6 nm) and PDI=0.112 (Figure S1C), (iii) in 0.1x PBS, average diameter was

1280.0 ± 71.48 nm and PDI= 0.214 (Figur S1D). These results indicate that the presence of complex biological fluids containing proteins, lipids and metabolites stabilizes the curcuminoid colloidal particle, resulting in smaller particle sizes in those aqueous environments.

3.3 TPNP in cell treatment media:

To evaluate whether TPNPs in cell-treatment media (RPMI-1640 with 0.5% FBS) changed particle size, TPNPs were diluted to make 50 µM curcuminoids equivalent in cell-treatment media and was found that average hydrodynamic diameter increased to 429.3 nm ± 14.6 nm with PDI = 0.225 (Figure S1E), whereas TPNP diluted in RPMI-1640 without FBS showed diameter of 140.6 ± 2.35 nm), PDI=0.179 (Figure S1F). These results may suggest that complex biological molecules present in FBS may form biological corona around the TPNPs.

3.4 Pharmaceutical equivalent curcuminoids loading of TPNP:

Curcuminoids loading capacity of TPNP and concentration of curcuminoids in standard Sigma curcumin were determined using High Performance Liquid Chromatograph equipped with an optical diode array detector (HPLC-DAD) with three individual curcuminoid standards (curcumin, Desmethoxycurcumin and Bisdemethoxycurcumin). HPLC-DAD analysis was also carried out for validation of a rapid spectroscopic assays developed.

Curcumin, desmethoxycurcumin, and bisdemethoxycurcumin were individually measured in HPLC and absorbance maximum at 429 nm, 423 nm and 419 nm, were

determined respectively (Figure S2A, S2B and S2C). Standard HPLC mass-fraction distribution of the three individual curcuminoid mixed together (100 ppm each) are shown in Figure S2D. HPLC results indicated that Sigma curcumin standard is composed of three curcuminoids (curcumin, Desmethoxycurcumin and Bisdemethoxycurcumin) and its actual pharmaceutical equivalent curcuminoids' concentrations were verified. Relative mass fraction distribution of three curcuminoids of Sigma curcumin standard and TPNP are shown in Figure- 2A and 2B respectively. The pharmaceutical equivalent total curcuminoids loading capacity of TPNP samples was found to be 2.03 mM by HPLC method.

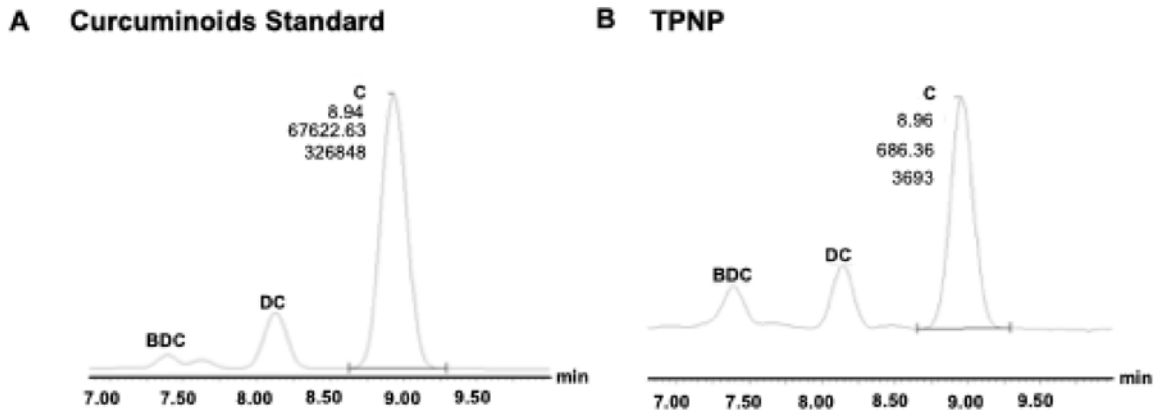

Figure-2

Fig-2: (A) Relative mass fraction distribution of three species of curcuminoids [curcumin (Cu), desmethoxycurcumin (DC) and bisdemethoxycurcumin (BDC)] in standard Sigma curcumin used, (B) Relative abundance of Cu, DC and BDC as mass fraction distribution of curcuminoids in TPNP. The numbers on the Cu peaks are (top to bottom) Retention time in minutes, peak area and peak height respectively).

For a rapid and inexpensive 96-well assay, the standard Sigma curcumin forming CSAP and TPNP prepared in 0.1x PBS to identify maximum absorbance wavelength and scanned from 250 nm to 800 nm at 1 nm interval. The absorbance maximum was found to be about 430 nm for both the samples (Figure S 3A, 3B), meaning the highest absorbing light to standard curcumin and TPNP is about 420-430 nm in agreement to published literature [50], but was found to be not very sensitive. A more sensitive rapid assay was developed using fluorescent spectroscopic method to quantify total curcuminoids in samples, which was further validated HPLC. For fluorescent spectroscopy assay the standard Sigma curcumin stock and TPNP were diluted in 80% ethanol followed by measurement with fluorescent excitation at 420 nm and emission capture at 570 nm. Based on HPLC spectra, 420 nm was selected as a common excitation wavelength for all three curcuminoids, as it provides near-maximal absorbance for all three species and is suitable for use in fluorescence spectroscopy assays. The rational of using 80% ethanol as a dilutant for fluorescent spectroscopy is to liberate all curcuminoids from the TPNP and CSAP into the solution for spectral measurements and to limit self-aggregating particles. Using fluorescent excitation at 420 nm and emission capture at 570 nm a pharmaceutical equivalent curcuminoids concentration standard curve was built (Figure S 3C) for further batch-to-batch curcuminoid load measurements.

Using fluorescent based method, the pharmaceutical equivalent curcuminoids concentration of TPNP samples used in *in vitro* work was measured to be 1.91 mM, whereas 2.03 mM by HPLC method. Validation by HPLC-DAD showed that fluorescent spectroscopy (combined with 80% ethanol for particles disruption) measured total curcuminoid content with a margin of error within 6%, supporting its use as a reliable method for quantifying total curcuminoids in the TPNP sample batches used in this study.

The dry weight of TPNP samples were determined to be 2877.6 µg / mL and found to contain 715 µg / mL total curcuminoid (Sum of curcumin, desmethoxycurcumin and bisdemethoxycurcumin concentrations determined by HPLC-DAD), indicating about 24.85% curcuminoid loading capacity (mass x mass) in the TPNP samples.

The particle concentration of TPNP was 9.58 x 10^{10} /mL, with a corresponding dry weight of 2877.6 µg/ml. Based on these values, the average dry weight of a single TPNP was estimated to be approximately 30.29 fg (femtogram), of which ~7.5 fg corresponds to curcuminoids; the remaining mass consists of molecules derived from the same turmeric rhizomes.

3.5 Antioxidant capacity

Curcuminoids and other polyphenols are known to exhibit potent antioxidant capacity. The measurement of antioxidant capacity by Ferric Reducing Antioxidant Power (FRAP) assay for TPNP and standard Sigma curcumin was performed, where NAC (N-acetycysteine) and Gallic Acid (GA) served as reference antioxidants. To calculate % antioxidant capacity, 62.5 µM curcuminoids (Sigma) was use as 100% reference point and compared with (i) TPNP (curcuminoid equivalent 62.5 µM), (ii) 62.5 µM NAC and (iii) 62.5 µM GA, as shown in Figure 3A. The TPNP suspension medium or vehicle showed no antioxidant activity. The antioxidant capacity observed at the 62.5 µM curcuminoid equivalent dose of TPNP, approximately 2.6 times greater than that of 62.5 µM standard Sigma curcumin (Figure- 3B), may be attributed to the presence of other polyphenols sourced from the biomass of turmeric rhizome, which comprises approximately 75% of the total mass.

A

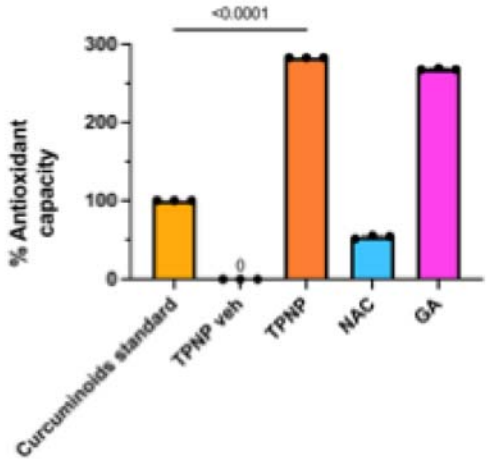

B

Reference-Based Total Antioxidant Capacity

Sample	Average OD of Fe^{2+}-TPTZ @560nm	Average Fe^{2+}-TPTZ µM
Curcuminoids standard	0.222	141
TPNP veh	0	0
TPNP	0.587	400
NAC	0.129	75.6
GA	0.557	379

*All to reference of 62.5 μM_{eq} Curcuminoids Standard

Figure-3

Fig-3: Ferric Reducing Antioxidant Power (FRAP), a colorimetric assay designed for the quantification and detection of Ferric Antioxidant Status on 62.5 µM equivalents of Sigma curcumin, TPNP, N-Acetyl-L-Cysteine (NAC), and gallic acid (GA). (A) displays percent antioxidant capacity or FRAP and (B) values of optical density (OD) and corresponding Fe^{2+} concentrations.

3.6 Dose tolerance of pharmaceutical equivalent concentration CSAP and TPNP in THP-1 monocyte / macrophages cells:

Titration of CSAP and TPNP doses were performed to identify LD_{50} (Figure-4). As shown in Figure- 4A and 4B, THP-1 monocytes were treated with varying doses of standard curcuminoids (forming CSAP in RPMI-1640-supplemented with 0.5% FBS) as well as TPNP in cell culture media followed by cellular viability analysis, which was measured by resazurin method. In monocytes, the LD_{50} of the standard curcuminoids-based CSAP was approximately 9.24 µM, whereas that of TPNP was higher, at 12.0 µM. We conducted a similar cell viability study in THP-1 macrophages (differentiated from THP-1 monocytes as described in method section) by exposing the differentiated

cells to varying doses of CSAP and TPNP, and observed an LD_{50} of 10.3 µM for both CSAP and TPNP treatments (Figure 4C and 4D).

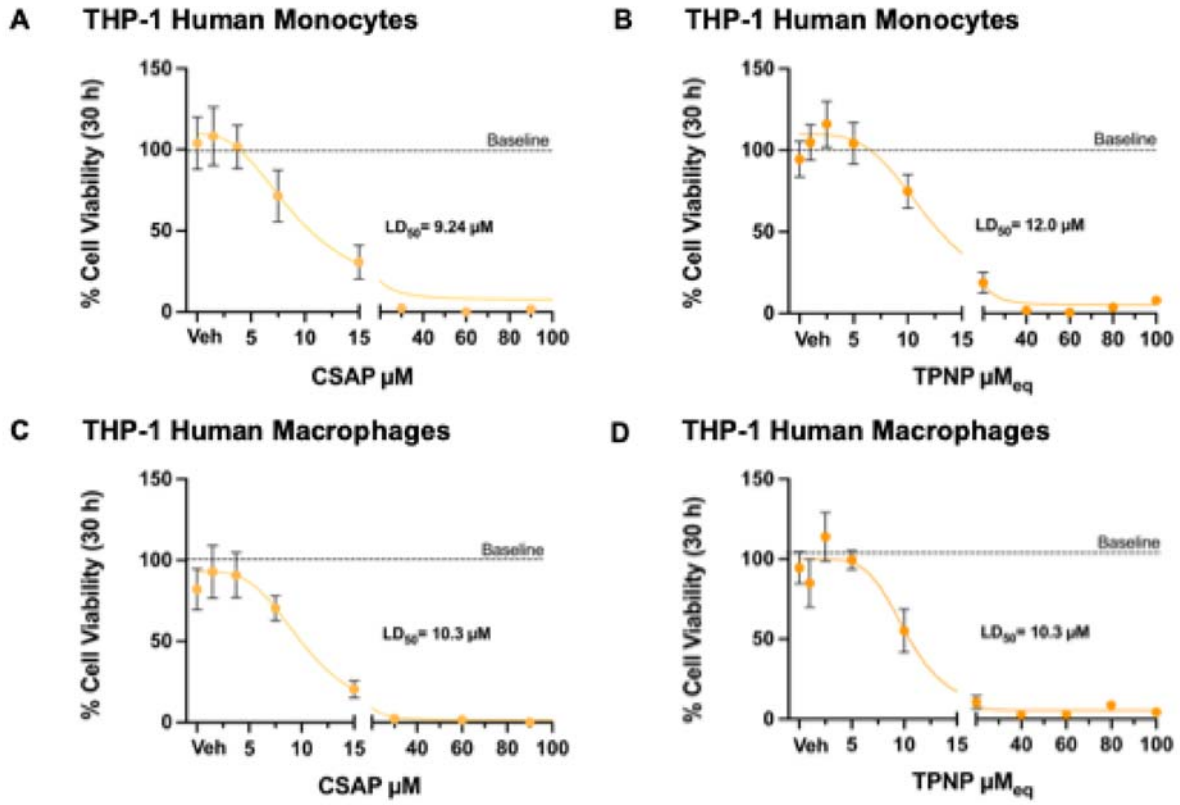

Figure-4

Fig-4: Cell viability assay to determine dose tolerance of standard Sigma curcumin spontaneous aggregation particle (CSAP) and TPNP in THP-1 monocyte and macrophages cells. (A) CSAP treatments on monocytes, (B) TPNP treatments on monocytes, (C) CSAP treatments on macrophages, (D) TPNP treatments on macrophages. Treatment concentrations were expressed as µM curcuminoids.

Two sub-lethal pharmaceutical doses curcuminoid equivalents of CSAP (3.75 µM and 7.5 µM) and TPNP (2.5 µM and 5.0 µM) was chosen to evaluate cellular survival in other non-immune cell types; human cardiomyocyte (AC16) and human blood brain barrier (BBB) cells (hCMEC/D3) as shown in Figure S4A & S4B respectively. Human AC16 cardiomyocytes were found to be less tolerant to high CSAP doses of 7.5 µM in

comparison to 3.75 µM whereas human Blood Brain Barrier cells TPNP were found to be well tolerated in these cells at 3.75 µM and 5.0 µM curcuminoids.

3.7 Bioavailability of CSAP and TPNP in THP1 monocytes and macrophages:

The internalization and accumulation of TPNP were observed using confocal microscopy where TPNP localization (autofluorescence of curcumin detected in the GFP channel), DAPI staining for nucleus (blue) and F-actin (Phalloidin-staining, red) were performed on THP1 macrophages and found to be comparatively enriched into nucleus than cytoplasm (Figure S5). TPNP curcuminoids doses of 7.5 µM and 5.0µM were selected to evaluate cellular uptake kinetics using Fluorescence-Activated Cell Sorting (FACS). Higher dose of CSAP (7.5 µM curcuminoid) were selected to obtain optimal FACS fluorescence signal to difference between curcuminoid positive and unstained cells with minimum background. As shown in Figure 5A, 5B(i) and Table S1, THP-1 macrophages were treated with standard pure curcuminoids derived CSAP (7.5 µM curcuminoid) and TPNP (5.0 µM curcuminoid). TPNP (5.0 µM curcuminoid) internalized rapidly by these cells, accumulating in 47.5% of cells (median fluorescent intensity= 527) within 30 min of exposure and progressively accumulating in 95.3% of cells (median fluorescent intensity= 1271) at 16 h whereas standard pure curcuminoids derived CSAP (7.5 µM curcuminoid) dose accumulating in only about 8.05% of cells (median fluorescent intensity=277) within 30 min of exposure and reaching 28.8% of cells (median fluorescent intensity= 423) at 2 h of exposure followed by progressively less cells containing standard pure curcuminoids as shown Figure 5B(i) and Table S1.

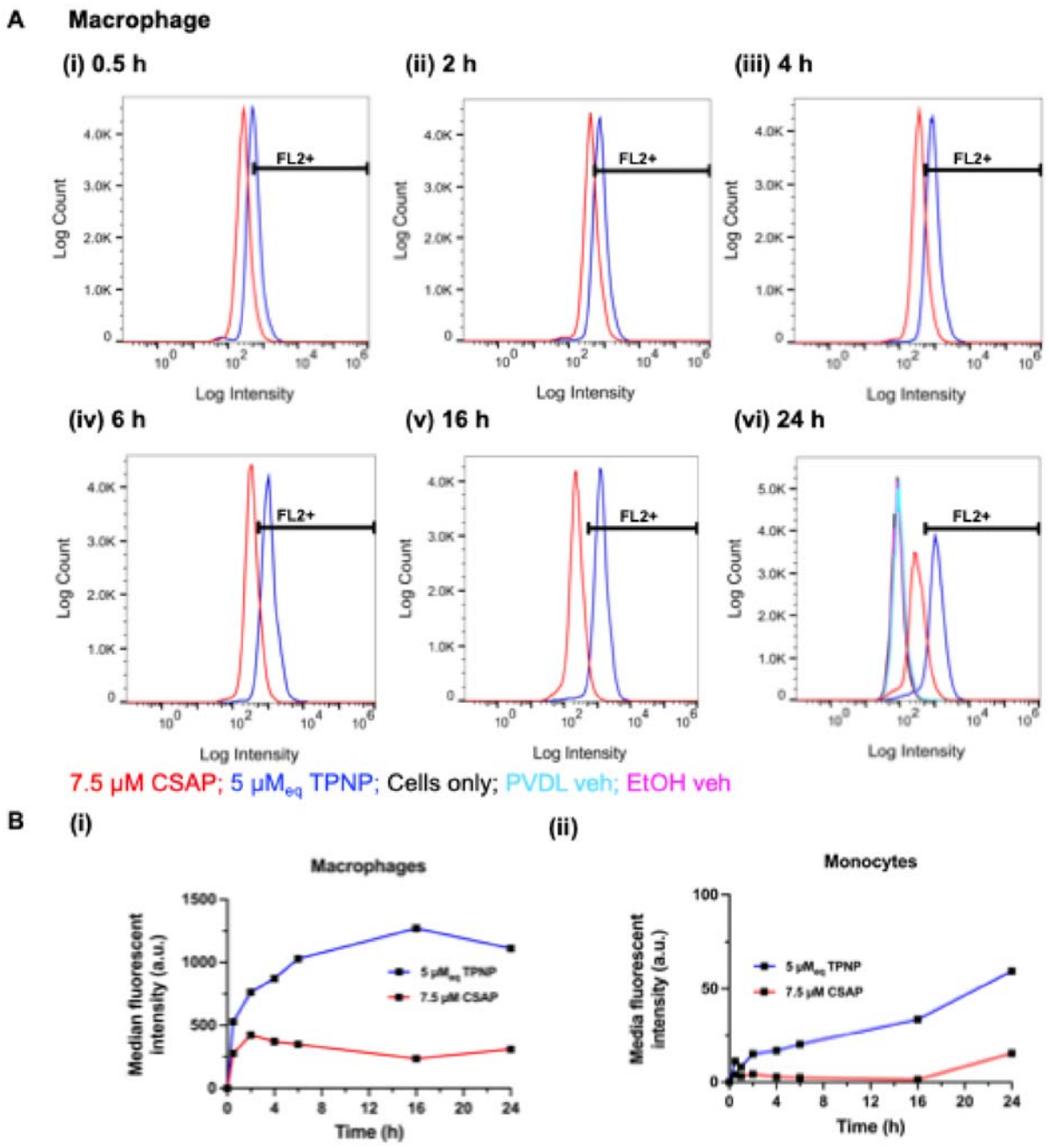

Figure-5

Fig-5: (A) A representative comparative-bioavailability kinetics of CSAP and TPNP in THP1 macrophages at 0.5h, 2h, 4h 6h, 16h and 24h time points. PVDL veh means vehicle of TPNP. (B) Median fluorescent intensity of gated (i) macrophages and (ii) monocytes positive for curcuminoid fluorescence signal over time.

Similarly, THP-1 monocytes were treated with CSAP (7.5 µM curcuminoid) and TPNP (5.0 µM curcuminoid) pharmaceutical doses for up to 24 h, Figure 5B(ii), Figure S6 and Table S2. FACS analysis demonstrated the accumulation/internalization of TPNP (5.0 µM curcuminoid) in monocytes reaching 16.9% cells (median fluorescent intensity= 739) after 4 h of exposure and highest at 59.4% of cells (median fluorescent intensity= 1397) after 24 h of exposure, whereas standard pure curcuminoids derived CSAP (7.5 µM curcuminoid) dose accumulating to 2.85% (median fluorescent intensity= 313) in 4h and highest about 15.4% of cells (median fluorescent intensity= 659) after 24h of exposure (Figure S6, Table S2). TPNP was internalized more rapidly than CSAP in both macrophages and monocytes, which may indicate that TPNP formulation is better for cellular bioavailability compared to CSAP.

3.8 Cellular pharmacodynamic anti-inflammatory effects of TPNP:

Cellular pharmacodynamic is estimation of pharmacological actions on living cells and its manifestation of the actions of the pharmaceutically important compounds.

3.8.1. Anti-inflammatory enzyme HMOX1 expression increases with treatments of TPNP in THP-1 monocytes and macrophages:

Increased expression of HMOX1 correlates with anti-inflammatory effects and promote wound healing in damaged tissues. Here we evaluated HMOX1 enzyme expression using immunoblotting in THP-1 monocytes (Figure 6A). HMOX1 enzyme expression were evaluated with treatments (4.5 h) of TPNP (5.0 µM curcuminoid) doses and standard pure curcuminoids derived CSAP curcuminoid dose of (7.5 µM). No HMOX1 enzyme expression was observed in control treatments, but relatively higher expression

was observed with TPNP (5.0 µM) than standard pure curcuminoids derived CSAP (7.5 µM curcuminoid). The total MemCode protein stain confirms equal protein loading across samples. Hemin (5.0 µM) used as positive control of HMOX1 enzyme expression.

Similarly, THP-1 macrophages were treated for 6 h with TPNP curcuminoid doses (5.0 µM) and standard pure curcuminoids derived CSAP (7.5 µM curcuminoid) and immunoblotted for HMOX1 enzyme expression. As shown in Figure 6B, TPNP induce more HMOX1 enzyme expression in macrophages at lower curcuminoid dose in comparison to higher dose of standard pure curcuminoids derived CSAP. Respective vehicle treated and untreated control cells showed basal level of HMOX1 enzyme expression, with the total MemCode protein stain confirming uniform protein loading across samples.

3.8.2. Dampening of LPS induced inflammation with treatments of TPNP in THP1 macrophages: Curcuminoids are known to downregulate levels of TNF-α. THP-1 macrophages responded to LPS stimulation by quickly releasing TNF-α in the media [52]. THP-1 macrophages were pre-treated with 5 µM curcuminoid TPNP or CSAP followed LPS (50 ng/mL) treatment at 0.5 h to induce inflammatory responses for a period of 1.5 h and 4 h. As shown in Figure 6C, the concentrations of TNF-α detected in the conditioned media demonstrating that TNF-α is a rapidly released pro-inflammatory cytokine, measurable in the conditioned media within 1.5 h of LPS exposure. Treatment with 5µM curcuminoid dose of TPNP or CSAP on LPS challenged macrophages reduced total secretion of TNF-α in comparison to media and vehicle controls. TPNP demonstrated superior reduction in TNF-α secretion when compared to CSAP at the

timepoint of 1.5 h (p=0.0393) and 4 h (p=0.0003). No significant reduction in TNF-α release was observed when THP-1 monocytes were subjected to the same treatment conditions and same LPS stimulation (data not shown).

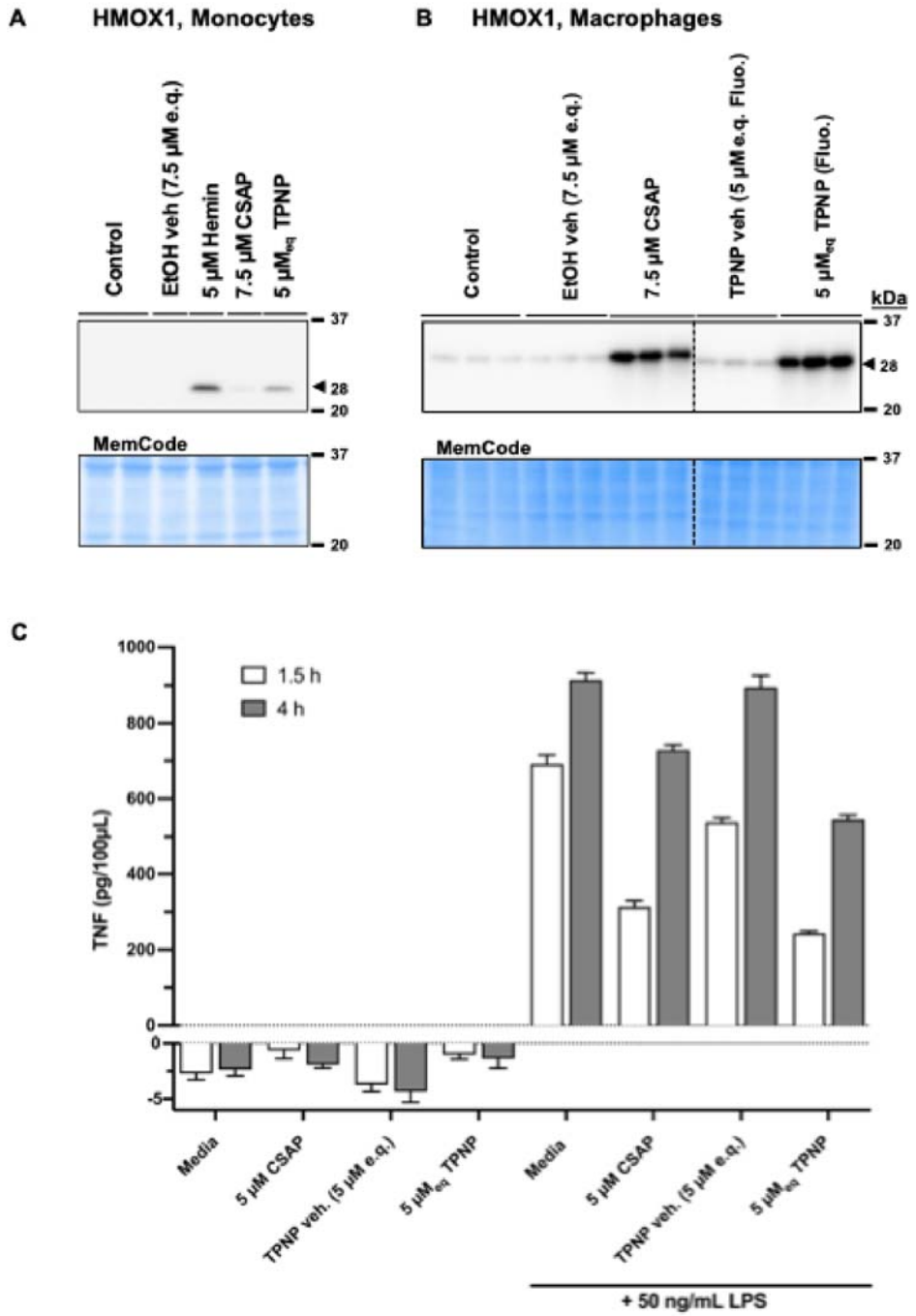

Figure-6

Fig-6: Immunoblotting of Human Heme Oxygenase-1 (HMOX1) on cells treated with indicated TPNP, CSAP, vehicle control and media only. (A) HMOX1 expression in

monocytes (Hemin was used as a positive control), (B) HMOX1 expression in macrophages following indicate treatments. **(C)** TNF-α concentration (pg/100 ul) in the conditioned media of treated macrophages with indicated time and treatment regimes.

4.0 Discussion

TPNPs are not plant-derived exosomes or vesicles or any sub-cellular structures originally synthesized within plant cells and tissues. Instead, they are manufactured as bio-native micelle-type structures enriched with curcuminoids directly from turmeric rhizomes, containing 24.85% curcuminoids by mass, with the remaining mass composed of endogenous molecules originally present in turmeric rhizomes. In this study, this novel class of all-natural, emulsion-free, surfactant-free, carrier-oil free Turmeric Phyto-Nanoparticle (TPNP) was evaluated alongside with Curcuminoids Spontaneous Aggregating Particles (CSAP), which formed in cell culture media under emulsion-free, surfactant-free, and carrier-oil-free conditions. Both TPNP and CSAP exhibited sub-micron hydrodynamic diameters. To confirm nanoparticles average hydrodynamic diameters two methods of biological nanoparticle analysis (DLS and TRPS) were performed and hydrodynamic diameters of TPNP were observed to be same using both the methods. TPNP demonstrated stability as dried powder after freeze-drying and storage at room temperature. Powdered TPNP increase their size after rehydration but maintain excellent population homogeneity. The presence of complex biological materials such as FBS was found to influence the effective hydrodynamic diameters of both TPNP and CSAP which may be due to interaction of FBS ingredients or formation of a bio-corona. The pharmaceutical equivalent curcuminoids contents of each particle type was quantified using High-Performance Liquid Chromatography, with individual curcuminoid standards (curcumin, desmethoxycurcumin, and bisdemethoxycurcumin), as well as HPLC-validated fluorescence spectroscopy for total curcuminoid concentration for batch-to-batch analysis. Curcuminoids

and other plant polyphenol are known scavenger of free radicals. At same pharmaceutical equivalent curcuminoids concentration, antioxidant capacity of TPNP was observed significantly higher in comparison to standard Sigma curcuminoids. The higher antioxidant capacity of TPNP may be attributed to other molecules from turmeric rhizome.

Curcuminoids are known for dose specific altered outcome, for example cancer cells are susceptible to a certain dose whereas similar curcuminoid dose generally exerts protective effects in healthy cells. Here, THP-1 monocytes and macrophages treated with CSAP and TPNP exhibited cytotoxic effects at higher pharmaceutical equivalent curcuminoid concentration with comparable LD_{50} doses observed in monocytes, while TPNP was slightly better tolerated in macrophages.

Cellular bioavailability [51] kinetics is the final dynamic process-stage in which active compounds to internalized to engage target cellular signaling pathways and serves as a useful tool for readily assessing compound bioavailability. Most hydrophobic drug candidates (both natural and synthetic) suffer from poor bioavailability, prompting the development of delivery technologies such as nanoemulsions. Curcuminoids are fluorescent green and can be detected using standard GFP filters /or channels of fluorescent spectroscopy, microscopy and FACS, which are ideal for curcuminoid quantitation. FACS analysis showed that while both cell types internalized TPNP and CSAP, uptake was slower and less efficient in monocytes. In contrast, macrophages internalized TPNP in 95% of cells (median fluorescent intensity= 1271) compared to only 5.58% of cells (median fluorescent intensity= 236) for CSAP at 16hr. The reduced accumulation of CSAP in both monocytes and macrophages may partially be explained by lower LD_{50} of CSAP over TPNPs in THP-1 monocytes. In macrophage,

preferential uptake [52] of larger particle TPNP (429.3 nm ± 14.6 nm) in comparison relatively smaller CSAP (122.1 nm ± 0.6 nm) may influence enhanced uptake in cell culture media.

Turmeric extracts and curcuminoids are attributed to possess immunomodulatory and anti-inflammatory/anti-oxidant effects. Monocytes to macrophages differentiation dynamics and further pro-inflammatory M1 or anti-inflammatory M2 macrophage polarization is essential for tissue repair pathways in the event of infection and damage. Increased expression of HMOX1 correlates with M2 phenotype [53], which has been shown to exert anti-inflammatory effects and promote wound healing in damaged tissues. Both TPNP and CSAP induced HMOX1 protein expression, with macrophages showing stronger responses than monocytes.

Tumor Necrosis Factor Alpha (TNF-α) is a rapid-response cytokine released by immune cells under conditions of stress, infection, or injury. It is widely regarded as a master regulator of inflammation, initiating a cascade of inflammatory signaling pathways that underlie many chronic diseases. Therefore, suppression or inhibition of TNF-α release presents a promising strategy for the development of anti-inflammatory therapeutics. Upon LPS stimulation, macrophages produced TNF-α, which was significantly reduced by TPNP pre-treatment compared to CSAP at the same pharmaceutical equivalent curcuminoids dose.

TPNPs increased the intracellular delivery efficiency of active curcuminoids, suggesting that all-natural nanoparticle formulations may offer enhanced therapeutic potential without the adverse effects associated with synthetic emulsifying excipients commonly used in nano-curcuminoid delivery systems. TPNPs may be proposed as safer to conventional nanoemulsions and lipid-based nanocarrier.

Acknowledgement: This research is supported by MITACS, a Canada Govt. organization to connect academic researchers with business.

Supplementary Figure:

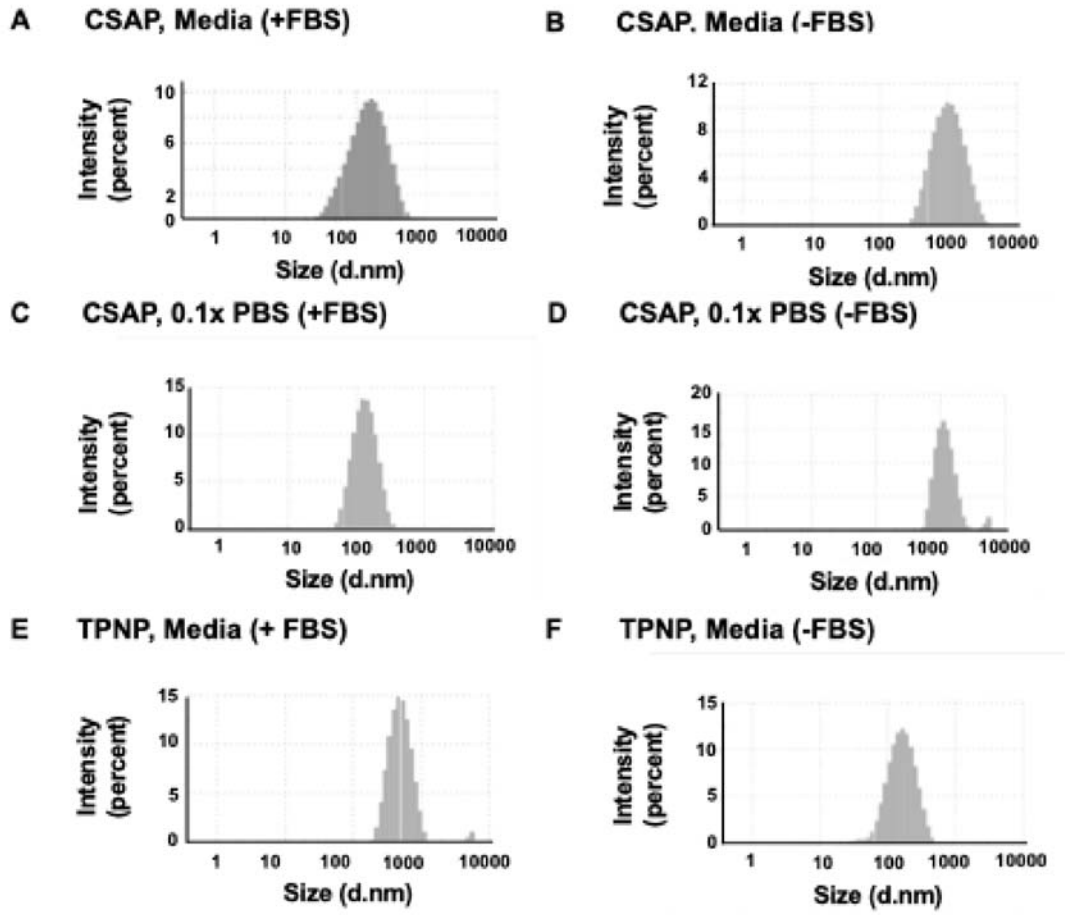

Figure S1

Figure S1: Particle size distribution of CSAP and TPNP in different aqueous media measured using DLS. (A) Particle size distribution of CSAP in RPMI-1640 media with 0.5% FBS, (B) Particle size distribution of CSAP in RPMI-1640 media without FBS, (C) Particle size distribution of CSAP in 0.1x PBS with 0.5% FBS, (D) Particle size distribution of CSAP in 0.1x PBS without FBS, (E) Particle size distribution of TPNP in RPMI-1640 media with 0.5% FBS, (F) Particle size distribution of TPNP in RPMI-1640 media without FBS.

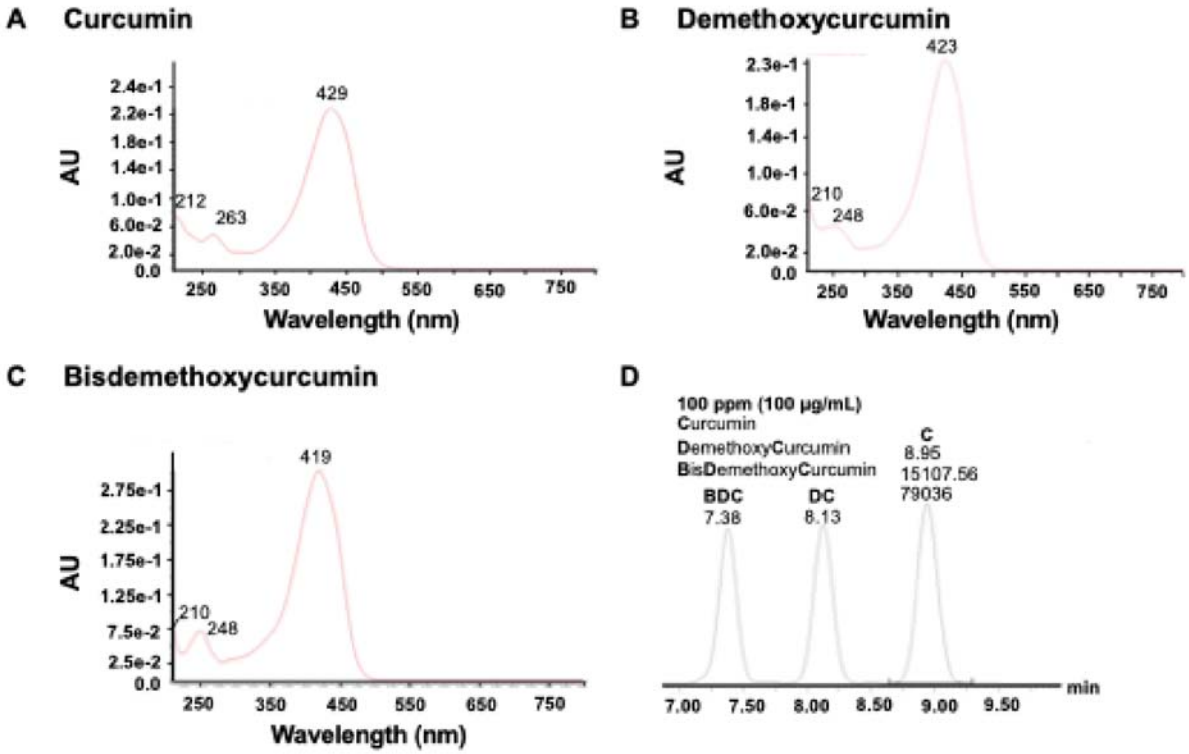

Figure S2

Figure S2: Representative HPLC absorbance graphs of 100 ppm of three species of curcuminoids separately: (A) curcumin, (B) desmethoxycurcumin and (C) bisdemethoxycurcumin. (D) Representative HPLC chromatograms showing 100 ppm equivalent mass fraction distributions of each of the three species of curcuminoids mixed together: curcumin (Cu), desmethoxycurcumin (DC) and bisdemethoxycurcumin (BDC). The numbers on the Cu peaks are (top to bottom) Retention time in minutes, peak area and peak height respectively and retention time of DC and BDC are also shown.

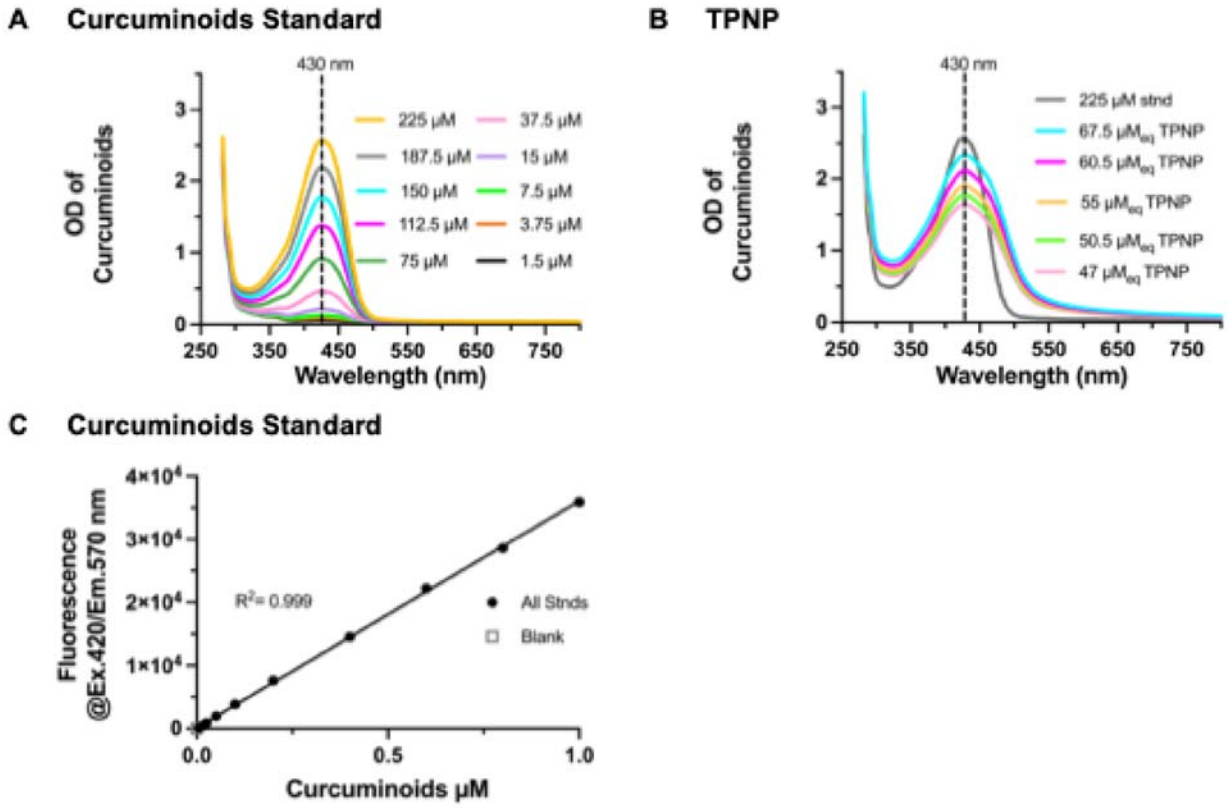

Figure S3

Figure S3: Absorbance spectra of different dilutions of (A) standard Sigma curcumin and (B) TPNP in water. (C) Standard curve of curcuminoids using fluorescent

spectroscopic method.

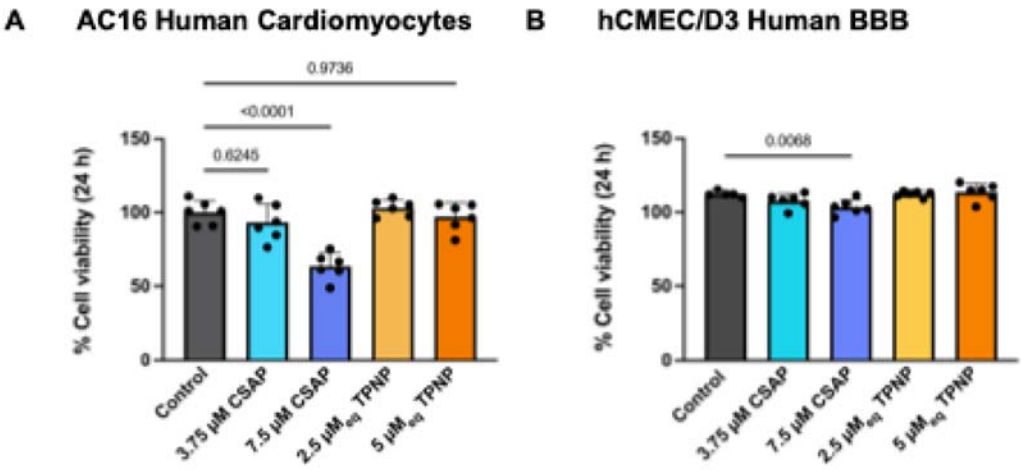

Figure S4

Figure S4: Cell viability assay to determine tolerance of standard Sigma curcumin spontaneous aggregation particle (CSAP) and TPNP as indicated in (A) human cardiomyocyte (AC16) and (B) human blood brain barrier (BBB) cells (hCMEC/D3).

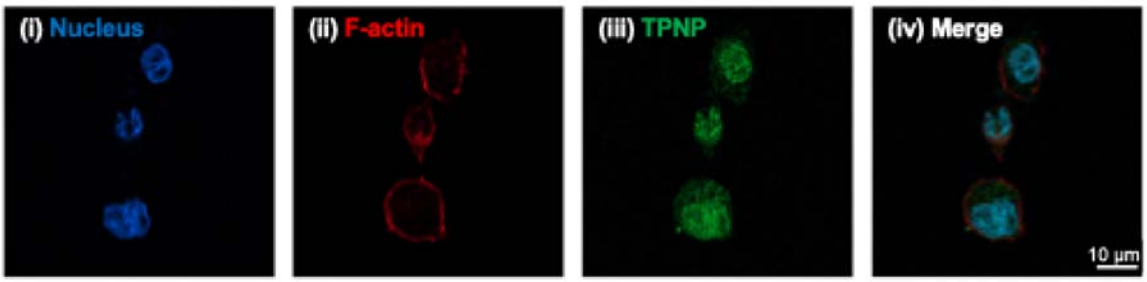

Figure S5

Figure S5: Relative abundance of TPNP in sub-cellular localizations of macrophages. (i) Nucleus (Hoechest, blue), (ii) F-actin (Phalloidin, red) (iii) TPNP (green), (iv) Merged images of three previous panels.

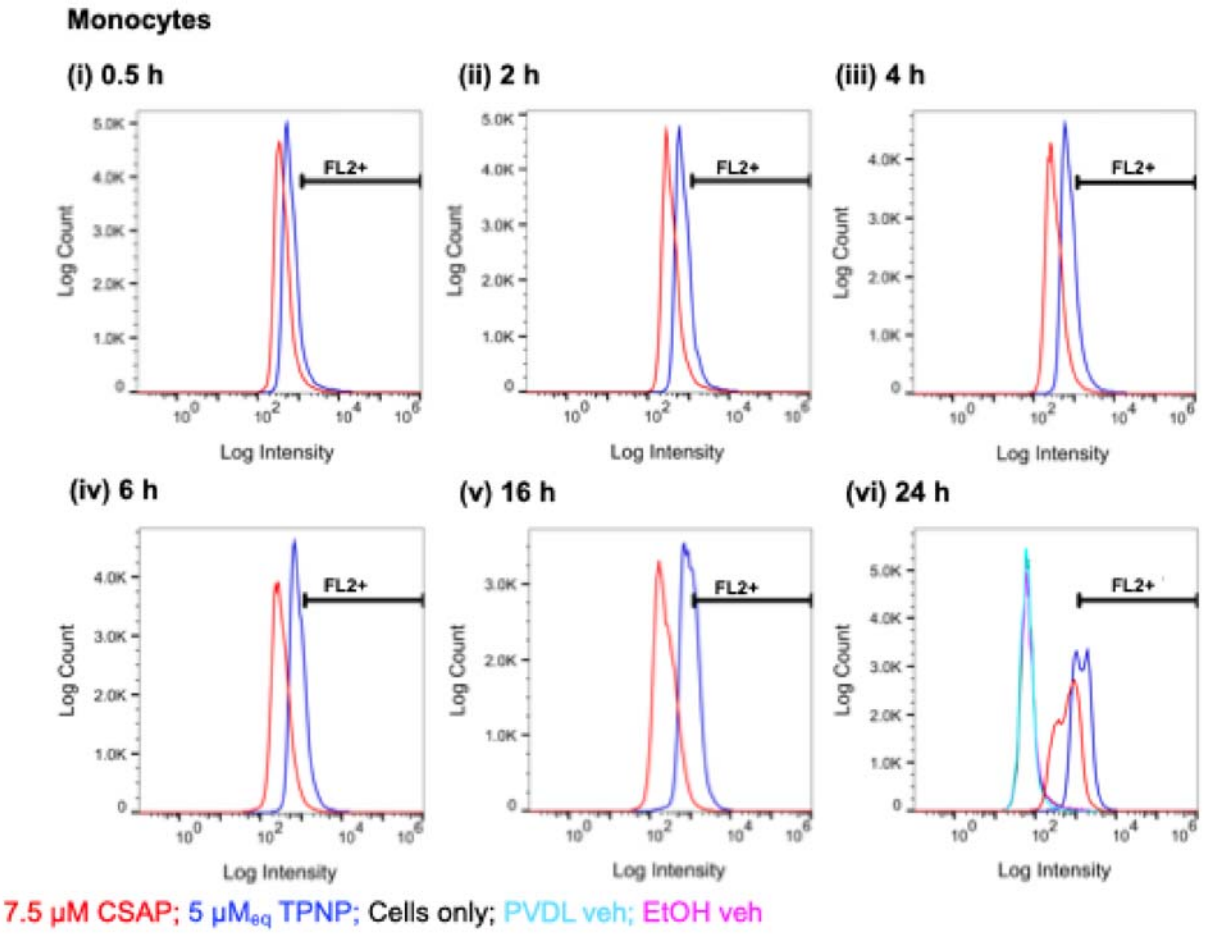

Figure S6

Figure S6: A representative FACS data of comparative-bioavailability kinetics of CSAP and TPNP in THP1 monocytes at 0.5h, 2h, 4h 6h, 16h and 24h time points. PVDL veh means vehicle of TPNP.

Table S1

Macrophages				
Sample	**Time (h)**	**% Total**	**Median**	**Gate (%)**
Media only	24	100	87.2	0.26
EtOH veh	24	100	92.1	0.41
PVDL veh	24	100	96.9	0.35
7.5 μM CSAP	0.5	100	277	8.05
	1	100	370	20.2
	2	100	423	28.8
	4	100	372	19.7
	6	100	349	17.4
	16	100	236	5.58
	24	100	310	16.9
5 μM_{eq} TPNP	0.5	100	527	47.5
	1	100	636	65.6
	2	100	763	79.6
	4	100	872	87.7
	6	100	1028	92.4
	16	100	1271	95.3
	24	100	1112	89.8

Table S1: Table summarizing Macrophage FACS data of percent of gated cells in the FL2 channel (curcuminoid positive) with indicated time of treatments with indicated CSAP and TPNP dose. PVDL veh means vehicle of TPNP.

Table S2

Monocytes				
Sample	**Time (h)**	**% Total**	**Median**	**Gate (%)**
Cells only	24	100	64.9	0.27
EtOH veh	24	100	63.9	0.70
PVDL veh	24	100	62.9	0.15
7.5 μM CSAP	0.5	100	389	4.08
	1	100	380	3.21
	2	100	345	4.28
	4	100	313	2.85
	6	100	303	2.51
	16	100	228	1.42
	24	100	659	15.4
5 μM_{eq} TPNP	0.5	100	622	11.2
	1	100	593	8.10
	2	100	710	15.0
	4	100	739	16.9
	6	100	803	20.2
	16	100	962	33.6
	24	100	1397	59.4

Table S2: Table summarizing Monocyte FACS data of percent of gated cells in the FL2 channel (curcuminoid positive) with indicated time of treatments with indicated CSAP and TPNP dose. PVDL veh means vehicle of TPNP.

Reference:

1. Jabczyk M, Nowak J, Hudzik B, Zubelewicz-Szkodzińska B. Curcumin in Metabolic Health and Disease. Nutrients. 2021 Dec 11;13(12):4440. doi: 10.3390/nu13124440. PMID: 34959992; PMCID: PMC8706619.
2. Peng Y, Ao M, Dong B, Jiang Y, Yu L, Chen Z, Hu C, Xu R. Anti-Inflammatory Effects of Curcumin in the Inflammatory Diseases: Status, Limitations and Countermeasures. Drug Des Devel Ther. 2021 Nov 2;15:4503-4525. doi: 10.2147/DDDT.S327378. PMID: 34754179; PMCID: PMC8572027.
3. Cifuentes M, Verdejo HE, Castro PF, Corvalan AH, Ferreccio C, Quest AFG, Kogan MJ, Lavandero S. Low-Grade Chronic Inflammation: a Shared Mechanism for Chronic Diseases. Physiology (Bethesda). 2025 Jan 1;40(1):0. doi: 10.1152/physiol.00021.2024. Epub 2024 Jul 30. PMID: 39078396.
4. Jin W, Botchway BOA, Liu X. Curcumin Can Activate the Nrf2/HO-1 Signaling Pathway and Scavenge Free Radicals in Spinal Cord Injury Treatment. Neurorehabil Neural Repair. 2021 Jul;35(7):576-584. doi: 10.1177/15459683211011232. Epub 2021 May 13. PMID: 33980059.
5. Zhong Y, Feng J, Fan Z, Li J. Curcumin increases cholesterol efflux via heme oxygenase□1□mediated ABCA1 and SR□BI expression in macrophages. Mol Med Rep. 2018 Apr;17(4):6138-6143. doi: 10.3892/mmr.2018.8577. Epub 2018 Feb 8. PMID: 29436680.
6. Shao S, Ye X, Su W, Wang Y. Curcumin alleviates Alzheimer's disease by inhibiting inflammatory response, oxidative stress and activating the AMPK pathway. J Chem Neuroanat. 2023 Dec;134:102363. doi: 10.1016/j.jchemneu.2023.102363. Epub 2023 Nov 19. PMID: 37989445.
7. Md. Rezaul Islam, Abdur Rauf, Shopnil Akash, Sadiya Islam Trisha, Akram Hossain Nasim, Muniya Akter, Puja Sutro Dhar, Hanan A. Ogaly, Hassan A. Hemeg, Polrat Wilairatana, Muthu Thiruvengadam, Targeted therapies of curcumin focus on its therapeutic benefits in cancers and human health: Molecular signaling pathway-based approaches and future perspectives, Biomedicine & Pharmacotherapy, Volume 170, 2024, 116034.
8. Rapti, E.; Adamantidi, T.; Efthymiopoulos, P.; Kyzas, G.Z.; Tsoupras, A. Potential Applications of the Anti-Inflammatory, Antithrombotic and Antioxidant Health-Promoting Properties of Curcumin: A Critical Review. Nutraceuticals 2024, 4, 562-595. https://doi.org/10.3390/nutraceuticals4040031
9. Servida S, Piontini A, Gori F, Tomaino L, Moroncini G, De Gennaro Colonna V, La Vecchia C, Vigna L. Curcumin and Gut Microbiota: A Narrative Overview with Focus on Glycemic Control. Int J Mol Sci. 2024 Jul 14;25(14):7710. doi: 10.3390/ijms25147710. PMID: 39062953; PMCID: PMC11277527.
10. Enayati A, Soghi A, Butler AE, Rizzo M, Sahebkar A. The Effect of Curcumin on the Gut-Brain Axis: Therapeutic Implications. J Neurogastroenterol Motil. 2023 Oct 30;29(4):409-418. doi: 10.5056/jnm23065. PMID: 37814431; PMCID: PMC10577457.
11. Saeed MEM, Yücer R, Dawood M, Hegazy MF, Drif A, Ooko E, Kadioglu O, Seo EJ, Kamounah FS, Titinchi SJ, Bachmeier B, Efferth T. In Silico and In Vitro

Screening of 50 Curcumin Compounds as EGFR and NF-κB Inhibitors. Int J Mol Sci. 2022 Apr 2;23(7):3966. doi: 10.3390/ijms23073966. PMID: 35409325; PMCID: PMC9000198.

12. Barinda AJ, Arozal W, Sandhiutami NMD, Louisa M, Arfian N, Sandora N, Yusuf M. Curcumin Prevents Epithelial-to Mesenchymal Transition-Mediated Ovarian Cancer Progression through NRF2/ETBR/ET-1 Axis and Preserves Mitochondria Biogenesis in Kidney after Cisplatin Administration. Adv Pharm Bull. 2022 Jan;12(1):128-141. doi: 10.34172/apb.2022.014. Epub 2020 Sep 19. PMID: 35517894; PMCID: PMC9012927.
13. Chen Q, Lin W, Tang Y, He F, Liang B, Chen J, Li H, Zhu H. Curcumin targets YAP1 to enhance mitochondrial function and autophagy, protecting against UVB-induced photodamage. Front Immunol. 2025 Mar 25;16:1566287. doi: 10.3389/fimmu.2025.1566287. PMID: 40201180; PMCID: PMC11975583.
14. Boozari M, Butler AE, Sahebkar A. Impact of curcumin on toll-like receptors. J Cell Physiol. 2019 Aug;234(8):12471-12482. doi: 10.1002/jcp.28103. Epub 2019 Jan 8. PMID: 30623441.
15. Yang M, Akbar U, Mohan C. Curcumin in Autoimmune and Rheumatic Diseases. Nutrients. 2019 May 2;11(5):1004. doi: 10.3390/nu11051004. PMID: 31052496; PMCID: PMC6566522.
16. Wang Y, Zhang H, Hua L, Wang Z, Geng S, Zhang H, Zeng Z, Zhao J, Wang X, Wang Y. Curcumin prevents Alzheimer's disease progression by upregulating JMJD3. Am J Transl Res. 2022 Aug 15;14(8):5280-5294. PMID: 36105064; PMCID: PMC9452350.
17. Vijayan V, Wagener FADTG, Immenschuh S. The macrophage heme-heme oxygenase-1 system and its role in inflammation. Biochem Pharmacol. 2018 Jul;153:159-167. doi: 10.1016/j.bcp.2018.02.010. Epub 2018 Feb 13. PMID: 29452096.
18. Amirhossein Sahebkar, Arrigo F.G. Cicero, Luis E. Simental-Mendía, Bharat B. Aggarwal, Subash C. Gupta, Curcumin downregulates human tumor necrosis factor-α levels: A systematic review and meta-analysis ofrandomized controlled trials, Pharmacological Research, Volume 107,2016,Pages 234-242, https://doi.org/10.1016/j.phrs.2016.03.026.
19. Niu, Y.; He, J.; Ahmad, H.; Shen, M.; Zhao, Y.; Gan, Z.; Zhang, L.; Zhong, X.; Wang, C.; Wang, T. Dietary Curcumin Supplementation Increases Antioxidant Capacity, Upregulates Nrf2 and Hmox1 Levels in the Liver of Piglet Model with Intrauterine Growth Retardation. *Nutrients* **2019**, *11*, 2978. https://doi.org/10.3390/nu11122978
20. Ziqiang Lin, Suo Wang, Yu Cao, Jialing Lin, Ailing Sun, Wei Huang, Jun Zhou, Qingxiong Hong, Bioinformatics and validation reveal the potential target of curcumin in the treatment of diabetic peripheral neuropathy, Neuropharmacology, Volume 260, 2024, 110131, ISSN 0028-3908, https://doi.org/10.1016/j.neuropharm.2024.110131.
21. Kushida T, Li Volti G, Quan S, Goodman A, Abraham NG. Role of human heme oxygenase-1 in attenuating TNF-alpha-mediated inflammation injury in endothelial cells. J Cell Biochem. 2002;87(4):377-85. doi: 10.1002/jcb.10316. PMID: 12397597.

22. Saqib U., Sarkar S., Suk K., Mohammad O., Baig M. S., Savai R. Phytochemicals as modulators of M1-M2 macrophages in inflammation. Oncotarget. 2018; 9: 17937-17950.
23. Stohs SJ, Chen O, Ray SD, Ji J, Bucci LR, Preuss HG. Highly Bioavailable Forms of Curcumin and Promising Avenues for Curcumin-Based Research and Application: A Review. Molecules. 2020 Mar 19;25(6):1397. doi: 10.3390/molecules25061397. PMID: 32204372; PMCID: PMC7144558.
24. Tabanelli, R.; Brogi, S.; Calderone, V. Improving Curcumin Bioavailability: Current Strategies and Future Perspectives. *Pharmaceutics* **2021**, *13*, 1715. https://doi.org/10.3390/pharmaceutics13101715
25. Panknin, T.M.; Howe, C.L.; Hauer, M.; Bucchireddigari, B.; Rossi, A.M.; Funk, J.L. Curcumin Supplementation and Human Disease: A Scoping Review of Clinical Trials. *Int. J. Mol. Sci.* **2023**, *24*, 4476. https://doi.org/10.3390/ijms24054476
26. Ajaikumar B. Kunnumakkara, Mangala Hegde, Dey Parama, Sosmitha Girisa, Aviral Kumar, Uzini Devi Daimary, Prachi Garodia, Sarat Chandra Yenisetti, Oommen V. Oommen, and Bharat B. Aggarwal. ACS Pharmacology & Translational Science 2023 6 (4), 447-518, DOI: 10.1021/acsptsci.2c00012.
27. Naghsh N, Musazadeh V, Nikpayam O, Kavyani Z, Moridpour AH, Golandam F, Faghfouri AH, Ostadrahimi A. Profiling Inflammatory Biomarkers following Curcumin Supplementation: An Umbrella Meta-Analysis of Randomized Clinical Trials. Evid Based Complement Alternat Med. 2023 Jan 16;2023:4875636. doi: 10.1155/2023/4875636. PMID: 36700039; PMCID: PMC9870680.
28. Mansouri, K., Rasoulpoor, S., Daneshkhah, A. *et al.* Clinical effects of curcumin in enhancing cancer therapy: A systematic review. *BMC Cancer* **20**, 791 (2020). https://doi.org/10.1186/s12885-020-07256-8
29. Miclotte L, De Paepe K, Rymenans L, Callewaert C, Raes J, Rajkovic A, Van Camp J, Van de Wiele T. Dietary Emulsifiers Alter Composition and Activity of the Human Gut Microbiota *in vitro*, Irrespective of Chemical or Natural Emulsifier Origin. Front Microbiol. 2020 Nov 5;11:577474. doi: 10.3389/fmicb.2020.577474. PMID: 33250870; PMCID: PMC7676226.
30. Naimi, S., Viennois, E., Gewirtz, A.T. *et al.* Direct impact of commonly used dietary emulsifiers on human gut microbiota. *Microbiome* **9**, 66 (2021). https://doi.org/10.1186/s40168-020-00996-6.
31. Eswar S, Rajagopalan B, Ete K, Nageswara Rao Gattem S. Serum Tumor Necrosis Factor Alpha (TNF-α) Levels in Obese and Overweight Adults: Correlations With Metabolic Syndrome and Inflammatory Markers. Cureus. 2024 Jul 15;16(7):e64619. doi: 10.7759/cureus.64619. PMID: 39149648; PMCID: PMC11326759.
32. De Siena, M.; Raoul, P.; Costantini, L.; Scarpellini, E.; Cintoni, M.; Gasbarrini, A.; Rinninella, E.; Mele, M.C. Food Emulsifiers and Metabolic Syndrome: The Role of the Gut Microbiota. *Foods* **2022**, *11*, 2205. https://doi.org/10.3390/foods11152205
33. Aaron S Bancil, Alicia M Sandall, Megan Rossi, Benoit Chassaing, James O Lindsay, Kevin Whelan, Food Additive Emulsifiers and Their Impact on Gut Microbiome, Permeability, and Inflammation: Mechanistic Insights in

Inflammatory Bowel Disease, *Journal of Crohn's and Colitis*, Volume 15, Issue 6, June 2021, Pages 1068–1079, https://doi.org/10.1093/ecco-jcc/jjaa254
34. Tan, Y.-B.; Wei, J.-Y.; Tang, Y.-F.; Ye, Y.-T.; Wang, L.; Yang, L.-J.; Chen, Z.-X. Effect of Ionic and Non-Ionic Surfactants on the Pasting Characteristics and Digestive Properties of Regular and Frozen Starch for Oral Delivery. *Foods* **2022**, *11*, 3395. https://doi.org/10.3390/foods11213395
35. Chassaing, B., Koren, O., Goodrich, J. *et al.* Dietary emulsifiers impact the mouse gut microbiota promoting colitis and metabolic syndrome. *Nature* **519**, 92–96 (2015). https://doi.org/10.1038/nature14232
36. Noubiap JJ, Nansseu JR, Lontchi-Yimagou E, Nkeck JR, Nyaga UF, Ngouo AT, Tounouga DN, Tianyi FL, Foka AJ, Ndoadoumgue AL, Bigna JJ. Global, regional, and country estimates of metabolic syndrome burden in children and adolescents in 2020: a systematic review and modelling analysis. Lancet Child Adolesc Health. 2022 Mar;6(3):158-170. doi: 10.1016/S2352-4642(21)00374-6. Epub 2022 Jan 17. PMID: 35051409.
37. Holder, M.K., Peters, N.V., Whylings, J. *et al.* Dietary emulsifiers consumption alters anxiety-like and social-related behaviors in mice in a sex-dependent manner. *Sci Rep* **9**, 172 (2019). https://doi.org/10.1038/s41598-018-36890-3
38. rnold, A.R., Chassaing, B., Pearce, B.D. *et al.* Dietary emulsifier consumption alters gene expression in the amygdala and paraventricular nucleus of the hypothalamus in mice. *Sci Rep* **12**, 9146 (2022). https://doi.org/10.1038/s41598-022-13021-7
39. Eskandani M, Hamishehkar H, Ezzati Nazhad Dolatabadi J. Cyto/Genotoxicity study of polyoxyethylene (20) sorbitan monolaurate (tween 20). DNA Cell Biol. 2013 Sep;32(9):498-503. doi: 10.1089/dna.2013.2059. Epub 2013 Jul 11. PMID: 23844597; PMCID: PMC3752516.
40. Kriegel, C.; Festag, M.; Kishore, R.S.K.; Roethlisberger, D.; Schmitt, G. Pediatric Safety of Polysorbates in Drug Formulations. *Children* **2020**, *7*, 1. https://doi.org/10.3390/children7010001
41. Lindenberg F, Sichel F, Lechevrel M, Respaud R, Saint-Lorant G (2019) Evaluation of Lung Cell Toxicity of Surfactants for Inhalation Route. J Toxicol Risk Assess 5:022. doi.org/10.23937/2572-4061.1510022
42. Arechabala B, Coiffard C, Rivalland P, Coiffard LJ, de Roeck-Holtzhauer Y. Comparison of cytotoxicity of various surfactants tested on normal human fibroblast cultures using the neutral red test, MTT assay and LDH release. J Appl Toxicol. 1999 May-Jun;19(3):163-5. doi: 10.1002/(sici)1099-1263(199905/06)19:3<163::aid-jat561>3.0.co;2-h. PMID: 10362266.
43. Silva, A.M.; Martins-Gomes, C.; Coutinho, T.E.; Fangueiro, J.F.; Sanchez-Lopez, E.; Pashirova, T.N.; Andreani, T.; Souto, E.B. Soft Cationic Nanoparticles for Drug Delivery: Production and Cytotoxicity of Solid Lipid Nanoparticles (SLNs). *Appl. Sci.* **2019**, *9*, 4438. https://doi.org/10.3390/app9204438
44. Vlachy N, Touraud D, Heilmann J, Kunz W. Determining the cytotoxicity of catanionic surfactant mixtures on HeLa cells. Colloids Surf B Biointerfaces. 2009 May 1;70(2):278-80. doi: 10.1016/j.colsurfb.2008.12.038. Epub 2009 Jan 6. PMID: 19201581.

45. Lam HT, Le-Vinh B, Phan TNQ, Bernkop-Schnürch A. Self-emulsifying drug delivery systems and cationic surfactants: do they potentiate each other in cytotoxicity? J Pharm Pharmacol. 2019 Feb;71(2):156-166. doi: 10.1111/jphp.13021. Epub 2018 Sep 25. PMID: 30251762.
46. Gong L, Zhu J, Yang Y, Qiao S, Ma L, Wang H, Zhang Y. Effect of polyethylene glycol on polysaccharides: From molecular modification, composite matrixes, synergetic properties to embeddable application in food fields. Carbohydr Polym. 2024 Mar 1;327:121647. doi: 10.1016/j.carbpol.2023.121647. Epub 2023 Dec 2. PMID: 38171672.
47. Hong L, Wang Z, Wei X, Shi J, Li C. Antibodies against polyethylene glycol in human blood: A literature review. J Pharmacol Toxicol Methods. 2020 Mar-Apr;102:106678. doi: 10.1016/j.vascn.2020.106678. Epub 2020 Jan 23. PMID: 31981619.
48. Allwood MA, Kinobe RT, Ballantyne L, Romanova N, Melo LG, Ward CA, Brunt KR, Simpson JA. Heme oxygenase-1 overexpression exacerbates heart failure with aging and pressure overload but is protective against isoproterenol-induced cardiomyopathy in mice. Cardiovasc Pathol. 2014 Jul-Aug;23(4):231-7. doi: 10.1016/j.carpath.2014.03.007. Epub 2014 Apr 5. PMID: 24813593.
49. Ghosh A, Kuppusamy H, Pilarski LM. Aberrant splice variants of HAS1 (Hyaluronan Synthase 1) multimerize with and modulate normally spliced HAS1 protein: a potential mechanism promoting human cancer. J Biol Chem. 2009 Jul 10;284(28):18840-50. doi: 10.1074/jbc.M109.013813. Epub 2009 May 18. PMID: 19451652; PMCID: PMC2707203.
50. Kang, S.; Kim, M.; Kim, H.; Hong, J. Enhancement of Solubility, Stability, Cellular Uptake, and Bioactivity of Curcumin by Polyvinyl Alcohol. *Int. J. Mol. Sci.* **2024**, *25*, 6278. https://doi.org/10.3390/ijms25116278
51. Teuscher KB, Zhang M, Ji H. A Versatile Method to Determine the Cellular Bioavailability of Small-Molecule Inhibitors. J Med Chem. 2017 Jan 12;60(1):157-169. doi: 10.1021/acs.jmedchem.6b00923. Epub 2017 Jan 3. PMID: 27935314; PMCID: PMC7771553.
52. Ivan S. Pires, Jack R. Suggs, Isabella S. Carlo, DongSoo Yun, Paula T. Hammond, and Darrell J. Irvine. Surfactant-Mediated Assembly of Precision-Size LiposomesChemistry of Materials 2024 36 (15), 7263-7273 DOI: 10.1021/acs.chemmater.4c01127
53. Funes SC, Rios M, Escobar-Vera J, Kalergis AM. Implications of macrophage polarization in autoimmunity. Immunology. 2018 Jun;154(2):186-195. doi: 10.1111/imm.12910. Epub 2018 Mar 8. PMID: 29455468; PMCID: PMC5980179.